

Numerical study of the effect of vitreous support on eye accommodation

DARJA LJUBIMOVA, ANDERS ERIKSSON

KTH Mechanics, Royal Institute of Technology, Osquars backe 18, SE-100 44 Stockholm, Sweden

SVETLANA BAUER

Saint-Petersburg State University, Department of Theoretical and Applied Mechanics,
Universitetsky pr. 28, 198504 Petergof, Russia

The aim of the current work was to extend previously created finite element models of accommodation such as the one by BURD [2] by addition of vitreous. The zonule consisted of anterior and central sets and vitreous was modelled as a linear elastic incompressible body. An inverse method was used to find some important, previously not documented, aspects. The model was found to behave according to the expectations, with results consistent with classical Helmholtz theory.

Key words: vitreous support, eye accommodation, finite element models

1. Introduction

Accommodation of an eye is the process of adjusting its focus distance to allow near objects to be focused on the retina. According to the widely accepted classical Helmholtz theory [19] and recent research in the accommodative apparatus of an eye [17], in the unaccommodated state the lens is flattened by the passive tension of the zonular fibres which are pulled by the elastic choroid structures. During accommodation the ciliary muscle contracts, thereby slides forward and towards the axis of the eye. It pulls the choroid structures, which causes the tension in the zonular fibres to reduce. With release of the resting tension of the zonular fibers, the elastic capsule reshapes the lens; it becomes more sharply curved and thickens axially. The equatorial diameter thereby decreases, increasing the refractive power of the eye.

It appears that in the improved description of the accommodative apparatus [17], anterior and posterior zonular fibres originate near ora serrata. From these observations one can conclude that the resultant of the tensile forces applied to the

ends of these zonular fibres is not horizontal at the equator but sloped posteriorly. It would contradict mechanical laws if such a construction did not have any support that is supplied by vitreous. It should be noticed that previous theoretical studies of accommodation [2], [14] assumed that all zonular fibres attach to the ciliary processes at a single point, which means that the resultant of stretching forces lies in an equatorial plane (figure 1a). These works did not include in the model the vitreous support, which should not be neglected.

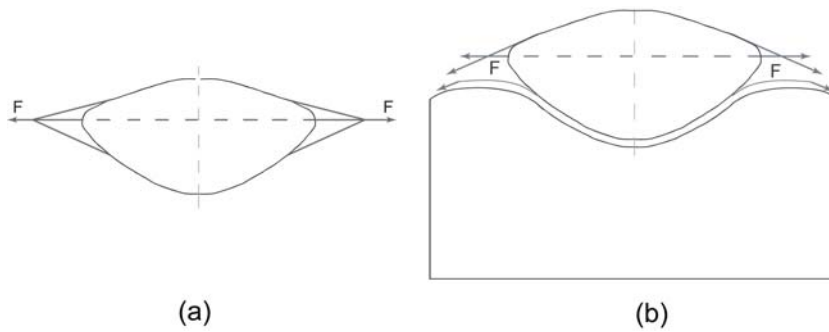


Fig. 1. Theoretical models: previous theoretical model [2], [14] (a), a new model (b)

We came to the conclusion that an improved theoretical model should consist of lens, zonular system and vitreous (figure 1b). The hypothesis of the present work is that an improved description of eye accommodation can be obtained by such a model.

In this study, we propose a finite element model of accommodation in which the effects of vitreous support are included. Some basic procedures established by BURD et al. [2] were used to model the accommodative lens and to perform post-processing, as described below. Since this is the first step in establishing an appropriate numerical model of the accommodative eye with the vitreous support, some reasoned assumptions were made to simplify the process and few of them have a noticeable influence on the behaviour of the model. These features were explored and are discussed in the paper. Our findings are of a preliminary nature and further work is necessary to develop a theoretical model that is capable of representing in detail the mechanism of accommodation of an eye.

2. Modelling process

An attempt was undertaken to study an accommodation of a 29-year-old eye. A numerical analysis has been carried out using the commercial general-purpose finite element package ABAQUS (ABAQUS Inc., USA) which is widely used in mechanical and civil engineering. The eye was regarded as being a body of revolution and an

axisymmetric analysis was adopted. Axisymmetric boundary conditions were applied to the nodes located along the symmetry axis. For the purpose of our study we adopted an assumption that all materials were isotropic and purely elastic [7]. Unfortunately, few published data are available to develop more complex material descriptions.

The present model involves complex contact simulation and the first-order elements are more appropriate in that case [3]. Such elements were chosen to avoid problems that usually appear in contact simulations when the second-order elements are used. Since triangular elements are geometrically versatile, it was convenient to use them meshing the interior of the lens, as it has a complex shape. Two-noded axis-membrane elements were used to model capsules of lens and vitreous to prevent the out-of-plane bending behaviour. We introduced the assumptions that interiors of the lens and vitreous are practically incompressible. It is known that it is better to use specially formulated elements (the so-called hybrid elements) to avoid problems associated with modelling incompressible materials. But since each hybrid triangular axisymmetric element introduces a constraint equation into an incompressible problem,

a mesh containing only these elements will be overconstrained. That was the reason we used normal axisymmetric elements for the lens and vitreous with Poisson's ratio of 0.49 representing near-incompressibility [3].

Lens. We assumed that the crystalline lens profile has the initial geometry, previously described in [2], and is composed of three layers, from surface to the center: capsule, cortex, nucleus. The variation in the thickness of capsule was provided in [9]. BURD et al. [2] developed the fifth-order polynomial using their data and these values were adopted in the present work to determine the axial stiffness of the membrane elements. Axisymmetric continuum three-noded elements were used to represent nucleus and cortex. Elastic moduli for capsule, cortex and nucleus were, respectively, 1.27 Nmm^{-2} [12], $3.417 \cdot 10^{-3} \text{ Nmm}^{-2}$ and $0.5474 \cdot 10^{-3} \text{ Nmm}^{-2}$ [8].

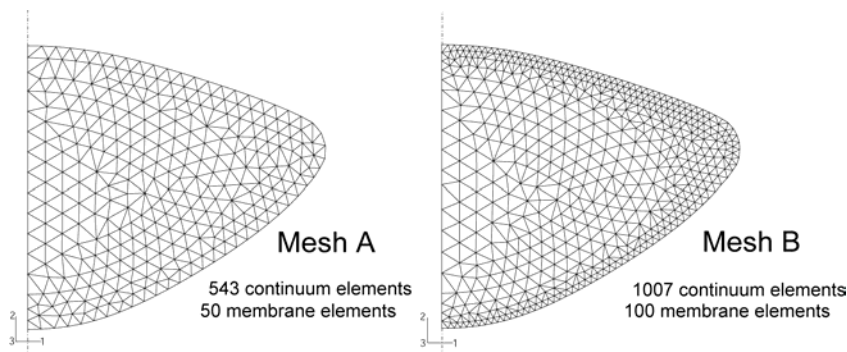


Fig. 2. Lens meshes: mesh with 593 elements (a), mesh with 1107 elements (b)

Two meshes were created for the crystalline lens to investigate the influence of mesh density on the results (figure 2). Here, we assumed that when the eye was in

a fully accommodated state (our reference configuration) all the stresses in the lens, capsules, vitreous and zonule were zero. An emphasis of the present work was given to the addition of the vitreous support to the model of accommodation. The assumptions of the reference state of the lens proposed in [2] were accepted. Therefore, questions about the relevance of these assumptions are still unresolved. These features are beyond the scope of the paper and left for the future research.

Zonule. The zonule is a supporting system for the lens. In a scanning electron microscope [6], [13], the zonule appeared to attach to the lens capsule in three distinct sets denoted by the places of their attachments to the lens: anterior, posterior and central. Each set of the zonule is composed of a number of individual fibrils, where anterior fibres (AFs) are more numerous than posterior fibres (PFs) and the number of central fibres is quite low. FISHER in [8] measured an angle α of inclination of the anterior zonular fibres to the lens axis, FARNSWORTH and SHYNE [6] reported the value for X —the distance between the anterior zonule attachment and the lens radius. We also use the assumption that central fibres (CFs) connect to the ciliary processes. STRENK et al. [16] obtained the reference value for ciliary body equator $R = 6.474$ mm. These values were adopted in our study (figure 3).

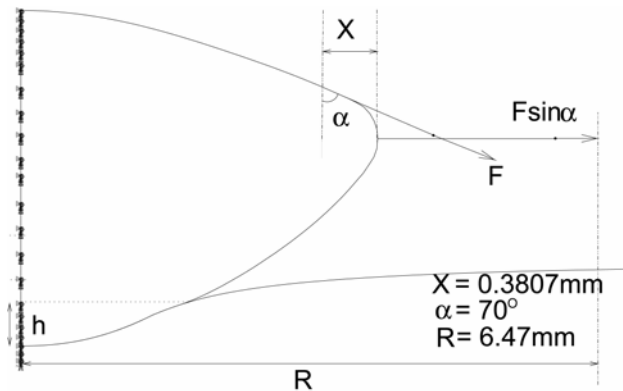


Fig. 3. Geometry of fully-accommodated eye

Addition of the vitreous support to the model complicates the simulations significantly due to the appearance of complex contact conditions (anterior fibres/lens capsule, posterior fibres/lens capsule, posterior fibres/vitreous). For the present modelling it was assumed that PFs together with Wieger's ligamentum and Berger's space could be neglected to simplify numerical analysis. It should be noticed that this assumption has a significant effect on the behaviour of the model. That feature is discussed later in the paper. Such an approach is considered to be satisfactory, since we put an emphasis on studying a certain aspect of accommodation, namely the "squeezing effect", which is achieved by stressed AFs and an additional stressed surface of the vitreous body in unaccommodated state.

It is difficult to specify the stiffness of zonule fibres since it depends on fibres number, size and elastic modulus. Van ALPHEN et al. [18] proposed a value of 1.5 Nmm^{-2} for Young's modulus of a zonule during their *in vitro* experiment of equatorially stretching lens. To determine the thickness which could not be found in literature, we performed an inverse experiment which is described below. We followed the assumption that the contact between the lens capsule and AFs was frictionless.

Vitreous. Traditionally the role of vitreous was neglected in accommodation. From a biomechanician's point of view, the vitreous body, which occupies the posterior compartment of the eye and is about 80% of the volume of the eyeball, represents a membrane full of vitreous humour. It maintains a certain level of intraocular pressure and ensures normal adjacency of the inside shells of an eye (choroid and retina). It is known that the vitreous membrane is quite elastic, a quality which keeps it under constant tension.

As a result, the vitreous body naturally tends towards spherical configuration, although the lens lying on the anterior part of the vitreous forms a small pit – fossa patellaris. To simplify the numerical analysis we replace the globular vitreous media by the rectangular one. It can be justified by the fact that effect of the far side of vitreous on the accommodation mechanism may be neglected. In the modelling, initial geometry of the vitreous was manually scaled from MR images [16]. We assumed that it is a nearly incompressible material with length and height of 10 mm and 17 mm, respectively. No information was found about mechanical properties of the vitreous and as the first approach we assumed that the vitreous humour and membrane are elastic materials. We modelled the membrane using two-noded axi-membrane elements. It was assumed that vitreous membrane has almost the same stiffness as the lens capsule with Young's modulus of 2 Nmm^{-2} and the thickness of 0.02 mm.

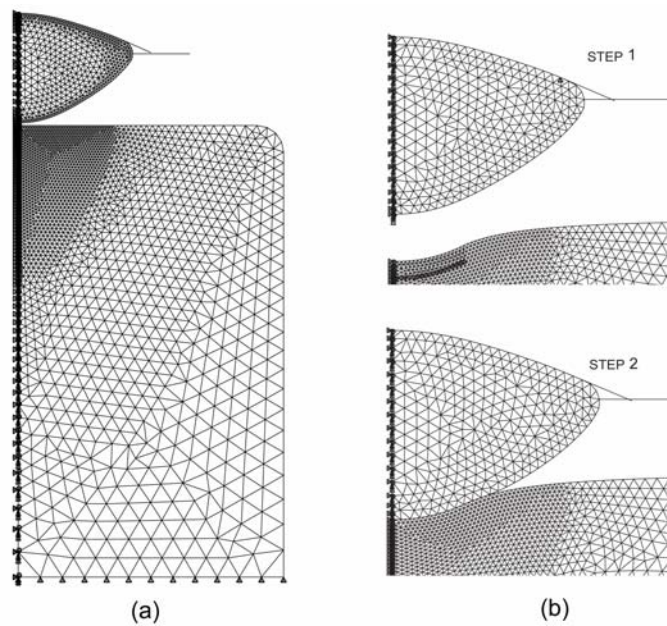


Fig. 4. Procedures: reference configuration, lens mesh B (a), preliminary steps with lens mesh A ($h = 1$) (b)

Procedure. The starting point of the simulation was lack of the contact between lens capsule and vitreous. The first step was done to achieve the configuration needed for simulation: to create fossa patellaris and to establish the contact between lens and vitreous avoiding the appearance of rigid body motions. The finite element model at its initial state is shown in figure 4a, and, after the preliminary step, in figure 4b.

In order to emulate stresses in vitreous which occur when we put the lens on the anterior hyaloid membrane, the first step was taken. Since the lens configuration was based on *in vivo* measurements [1], the shape of fossa patellaris should be the same as the shape of the posterior surface of the lens. To achieve this state we applied displacement boundary conditions. The depth h of the pit was unknown and we varied it from 1 mm to 3 mm (figure 3). The second step established the contact between vitreous body and lens capsule with a friction coefficient equal to $\mu = 0.01$ as for lubricated surfaces.

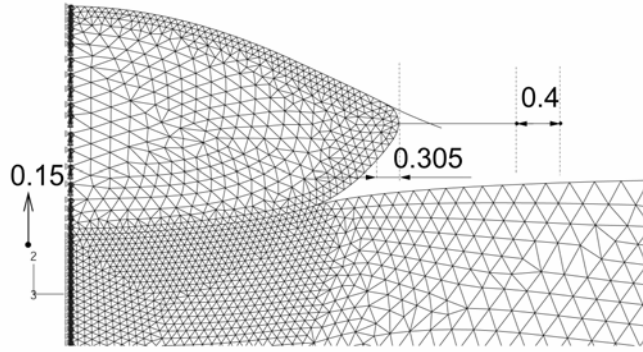


Fig. 5. Inverse experiment

Two simulations using different meshes were done by applying forces to the ends of the zonular fibres. To deduce unknown parameters (force, anterior and central zonule stiffness, Young's modulus of vitreous humour) we carried out inverse experiments. This is a well-known engineering methodology used to establish unknown parameters, by performing “what if” calculations in these parameters from which their values are deduced by comparing the resulting behaviour to the known factors. Finite element calculations were done by applying the outward tension to the ends of zonular fibres. It was assumed that the final deformed geometry should match the data reported in [1], [16] for non-accommodated state. STRENK et al. [16] suggest that when the ciliary body moves 0.4 mm, the corresponding change in lens equator radius would be 0.3 mm. BROWN [1] proposed that during disaccommodation the posterior pole moves 0.15 mm (see figure 5). Unknown parameters were manually adjusted at the end of each calculations to give the known deformed configuration.

3. Results

Calculations were performed and unknown parameters were calculated for different depths of fossa patellaris ($h = 1, 2, 3$ mm). We report data for configuration at $h = 2$ mm, other results are given in the “Sensitivity studies”. Solutions for lens geometry were found and each portion of the lens surface obtained was fitted with circular fits to calculate the anterior r_a and posterior r_p radii of curvature. A circular aperture of 0.6 mm radius was used, regarded as the optical zone and the most important for vision. A polar lens thickness (t) was calculated from the finite element simulation results. The optical power was determined based on the thick lens formula:

$$\text{Power}_{\text{lens}} = \frac{n - n_{av}}{r_a} + \frac{n - n_{av}}{r_p} - \frac{t(n - n_{av})^2}{r_a r_p n}.$$

We assumed refractive indices of $n_{av} = 1.336$ for aqueous and vitreous humour and $n_1 = 1.42$ for the crystalline lens, i.e., the values proposed for the Gullstrand–Emsley schematic eye. It should be noted that the procedure described here follows closely that described in [2].

During the simulation we manually deduced unknown parameters (force, Young's modulus of vitreous humour, zonular stiffness) by ensuring that the final geometry matched the data for the unaccommodated state of lens, as discussed above. At the values h considered, the final value of zonular force was 0.09 N and the thicknesses of anterior and central fibres were 70 μm and 29 μm , respectively.

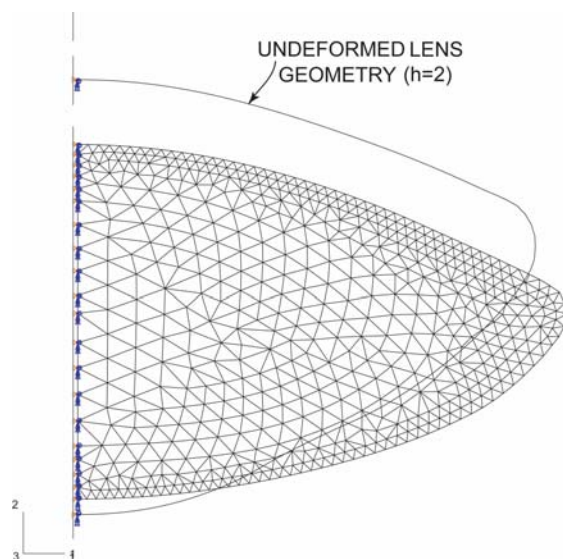


Fig. 6. Deformed mesh with 1107 elements for the lens

The deformed mesh for mesh B (see figure 2b) together with the reference lens surfaces is shown in figure 6. The simulations show that the central thickness of the crystalline lens increases with accommodation, and paraxial anterior and posterior curvatures become steeper.

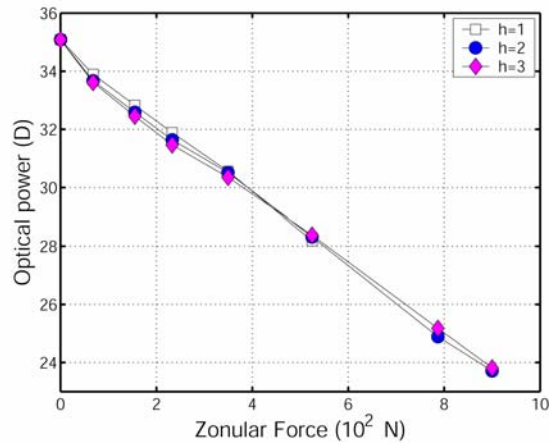


Fig. 7. Relationship between zonular force and optical power

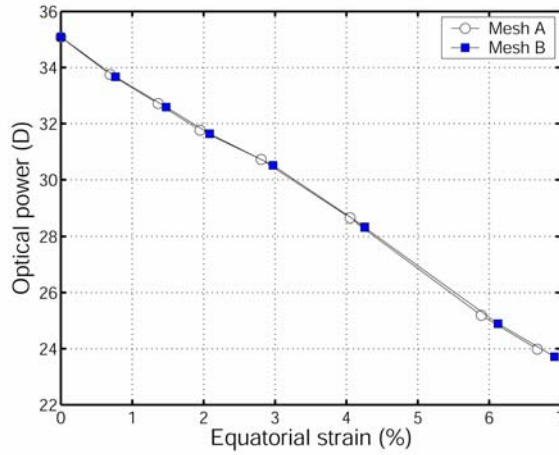


Fig. 8. Variation of optical power with equatorial strain

During disaccommodation, outward tension is applied to the lens and pulls it into a relatively flattened state, thus decreasing the lens power; these results are in agreement with the Helmholtz hypothesis of accommodation (figure 7). During stretching from accommodated to unaccommodated state, computed results indicated an 11% reduction in central anterior curvature and a 51% reduction in central posterior curvature. The corresponding decreases in optical power of the anterior and posterior surfaces were 2D and 10D, respectively, and the decrease in optical power of the whole lens was 11.3D. The decrease in geometric thickness during disaccommodation was 0.79 mm and occurred entirely in the nuclear region – 84%. This agrees well with measurements in [1]. The anterior pole moved backwards 0.6 mm, when the eye

changed its vision from near to far point, which is approximately three-quarters (76%) of the total change of lens thickness.

The computed variations of optical power with equatorial strain for two meshes with different densities are shown in figure 8. The difference in mesh densities has a small effect on the variation of the optical power. As the difference is limited the finer mesh B with 1107 elements is assumed to be acceptable.

4. Sensitivity studies

Since theoretical modelling critically depends on input parameters and assumptions, it is susceptible to errors. Any aspect of the model can be responsible for yielding poor-quality results. Thus, the effect of variability of different input data on performance of the model is an important question. Although the primary interest of this study was focused on the qualitative numerical analysis of accommodation process with vitreous support, some limited variations have been studied to decide the sensitivity of the results obtained.

Depth of fossa patellaris. Since the depth of fossa patellaris was unknown in our numerical simulations, three computational analyses with inversely estimated parameter values have been carried out for eye models with different depths of vitreous pit ($h = 1, 2, 3$ mm). It is clear from figure 9 that variation of h has noticeable effect on the behaviour of the model. Here we assumed that the values computed for zonular force of 0.09 N, anterior and central stiffness of 105 Nmm^{-1} and 43.5 Nmm^{-1} of the zonular fibers were the same for all three models.

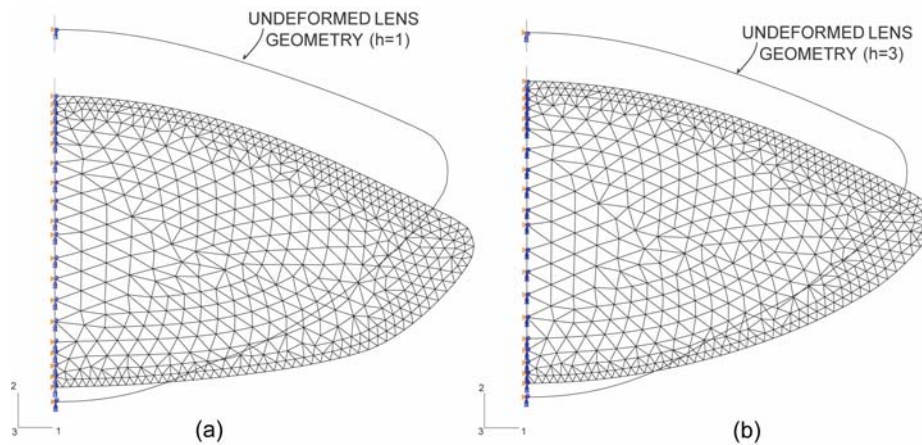


Fig. 9. Deformed mesh with different depths of pit: $h = 1$ (a), $h = 3$ (b)

During the process of disaccommodation, the posterior central curvature is flatter and the changes in thickness are greater for smaller values of h . This feature of the model would be expected on the basis that during calculations we fixed the

displacement of the posterior pole and lens equator and achieved the final configuration by varying the elastic modulus of the vitreous humour. Thus, for smaller h the vitreous substance was assumed to be stiffer with higher stresses during the second step of simulation (figure 4). As a consequence, the deformation of the posterior surface was greater during the contact. For $h = 1$, when the values of force exceeded 0.05 N, the posterior curvature varied so significantly with radius of circular aperture in the optical zone that we excluded these points from further consideration. Posterior curvatures for $h = 2, 3$ showed smooth behaviour during the analysis and these calculations were considered to be acceptable. The effect of difference in the depths of pit on radius of posterior curvatures of the lens is shown in figure 10.

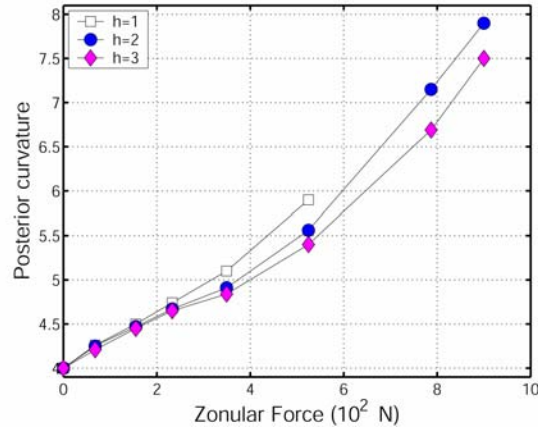


Fig. 10. Effect of difference in depths of pit on radius of posterior curvature of the lens

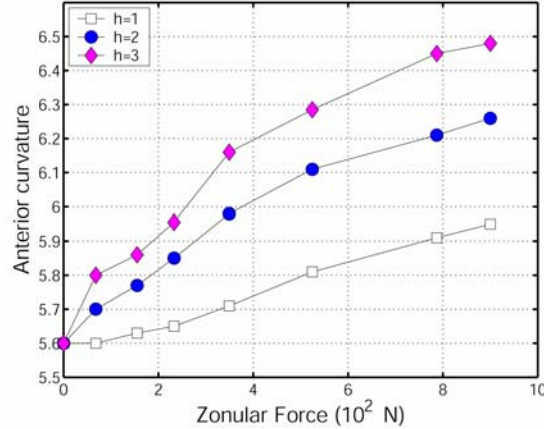


Fig. 11. Effect of difference in depths of pit on radius of anterior curvature of the lens

It is less clear from figure 9 how the anterior paraxial curvature changes. The computed results (figure 11) indicated greater increase in the anterior radius of

curvature with higher h , as the lens was stretched from accommodated to unaccommodated state (i.e. 6%, 11% and 14% for $h = 1, 2, 3$, respectively).

Incompressibility of the lens. Our calculations were based on the assumption that lens and vitreous matrix are incompressible. That means that Poisson's ratio should be equal to 0.5, which poses numerical difficulties during finite element simulations. Another calculation was carried out with Poisson's ratio inside the lens set to 0.499. We calculated the deformed volume, which should be constant for an incompressible material. For a computation at Poisson's ratio of 0.49 there is a loss in lens volume approaching 2% through the shortening process. For Poisson's ratio of 0.499 the volume is conserved. The difference in accommodation amplitude was about 5% between the cases, which is not considered significant.

5. Discussion

Classically it has been believed that the anterior lens surface is the main contributor to the accommodative process. Recently, partial coherence interferometry showed a posterior movement of the posterior surface, anterior movement of anterior surface and small forward translation of the center of mass of the lens [4]. It was reported that the forward movement of the anterior pole of the lens is approximately three times larger than the backward movement of the posterior pole during fixation from the far point to near point. According to our results the forward axial translation of the anterior surface is 76% of the increase in lens thickness, which is in agreement with [4], although polar movements are about three times as great as those observed by DREXLER et al. [4]. It should be mentioned that we fixed the posterior pole displacements on 0.15 mm [1], and [4] reported a value only one third of this.

In [1], it was shown with Scheimpffug slitlamp photography that the posterior curvature might increase, although the magnitude is unknown due to refraction by the lens and may be zero. We used the values given by BROWN [1] to recreate the initial geometry of the lens in our study, but it should be noted that because of optical distortions involved in this method [5], some inherent experimental errors can appear. GARNER and YAP [10] present measurements, showing that about one third of the change in lens power with accommodation of 8D is caused by the changes in posterior lens curvature. In our model, the change in optical power of the posterior surface was significantly greater than that in the anterior one. The posterior surface made not only substantial, but also main contribution to the overall increase in lens power with accommodation. It is expected for such a model because of the assumptions being accepted for the back of the lens. In reality, posterior surface of the lens adheres to the vitreous membrane creating Wieger's ligamentum, which includes a capsule-hyaloidal interspace, the so-called Berger's space. PFs have their origin in the line of attachment of the lens to the vitreous. The assemblage of these anatomical elements can be regarded as an additional annular sheet which is situated between the back of the lens

and vitreous membrane. It has certain stiffness and is confronting sudden changes of posterior curvature of the lens. In our model, this sheet is omitted to simplify the numerical analysis. During the contact simulation the lens is pressed into the vitreous by powerful AFs, thus producing major changes in posterior curvatures. Future models should include all anatomical components mentioned above to model the accommodative process even more precisely.

The computed variations of optical power with equatorial strain for two meshes with different densities were shown in figure 8. The picture shows that with an increase in the equatorial strain, optical power is reduced as predicted by classical theory, giving the average power reduction rate of approximately 1.6D per percent strain. STOREY and RABIE [15] report in their *in vivo* measurements a reduction of 1.2D per percent equatorial strain, GLASSER and CAMPBELL [11] show based on *in vitro* experiments that in young eyes the optical power of the lens is reduced at a rate between 0.7 and 1.25D per percent equatorial strain. These physiological measurements closely matched our results.

Since the movement of the posterior pole had the same fixed value for all calculations, the change in thickness occurred because of axial translation of the anterior pole. For the values of $h = 1, 2, 3$ the movements of the anterior surface were 0.733, 0.608, 0.555 mm, respectively. The resulting variation of optical power with zonular force for mentioned sets of analysis was shown in figure 7. It seems that different depths of pit had a small effect on the resulting optical power. That difference was regarded as being small enough to suggest that variation of fossa patellaris in our numerical exercise does not play a significant role and that the model is not sensitive to this parameter.

Computed results for the zonule stiffness satisfied the suggestion [18] that lens capsule and zonule are both three times as stiff as the lens substance.

6. Conclusions

Nonlinear finite element analysis was used to construct a numerical model of accommodation with vitreous support. It is not claimed that the model captures all physiological aspects of the accommodation, since some anatomical details are omitted. Better to say, it captures certain aspect of the mechanism, being the influence of vitreous, the so-called “squeezing” effect. The behaviour of the model seems to be in reasonable agreement with different published data. Accommodation of a young (not presbyopic) eye occurred similarly to the Helmholtz mechanism.

Further work is needed to develop a numerical model sufficiently close to the real process of accommodation of a 29-year-old eye. Better understanding of geometric and mechanical high-quality test data is required to calibrate more complex models. Some of these can be obtained or verified by an inverse methodology described in the paper. The research was partly supported by the RFBR Grant N 04-01-00258.

References

- [1] BROWN N., *The change in shape and internal form of the lens of the eye on accommodation*, Experimental Eye Research, 1973, 15, 441–459.
- [2] BURD H.J., JUDGE S.J., CROSS J.A., *Numerical modelling of the accommodating lens*, Vision Research, 2002, 42, 2235–2251.
- [3] COOK R.D., MALKUS D.S., PLESHA M.E., WITT R.J., *Concepts and applications of finite element analysis*, forth edition, John Wiley & Sons Inc, New York, 2002.
- [4] DREXLER W., BAUMGARTNER A., FINDL O., HITZENBERGER C.K., FERCHER A.F., *Biometric investigation of changes in the anterior eye segment during accommodation*, Vision Research, 1997, 37, 2789–2900.
- [5] DUBBELMAN M., van der HEIJDE G.L., *The shape of the aging human lens: curvature, equivalent refractive index and the lens paradox*, Vision Research, 2001, 41, 1867–1877.
- [6] FARNSWORTH P.N., SHYNE S.E., *Anterior zonular shifts with age*, Experimental Eye Research, 1979, 28, 291–297.
- [7] FISHER R.F., *The elastic constants of the human lens capsule*, Journal of Physiology, 1969, 201, 1–19.
- [8] FISHER R.F., *The elastic constants of the human lens*, Journal of Physiology, 1971, 212, 147–180.
- [9] FISHER R.F., PETTET B.E., *The postnatal growth of the capsule of the human crystalline lens*, Journal of Anatomy, 1972, 112(2), 207–214.
- [10] GARNER L.F., YAP M.K.H., *Changes in ocular dimensions and refraction with accommodation*, Ophthalmic and Physiological Optics, 1997, 17, 12–17.
- [11] GLASSER A., CAMPBELL M.C.W., *Biometric, optical and physical changes in the isolated human crystalline lens with age in relation to presbyopia*, Vision Research, 1999, 39(11), 1991–2015.
- [12] KRAG S., OLSEN T., ANDREASSEN T.T., *Biomechanical characteristics of the human anterior lens capsule in relation to age*, Investigative Ophthalmology and Visual Science, 1997, 38(2), 357–363.
- [13] LUDWIG K., WEGSHEIDER E., HOOPS J.P., KAMPIK A., *In vivo imaging of the human zonular apparatus with high-resolution ultrasound biomicroscopy*, Graefe's Archive for Clinical and Experimental Ophthalmology, 1999, 237(5), 361–371.
- [14] SCHACHAR R.A., BAX A.J., *Mechanism of human accommodation as analysed by nonlinear finite analysis*, Annals of Ophthalmology Clinics, 2001, 33(2), 103–112.
- [15] STOREY J.K., RABIE E.P., *Ultrasonic measurement of transverse lens diameter during accommodation*, Ophthalmic and Physiological Optics, 1985, 5, 145–148.
- [16] STRENK S.A., SEMMLow J.L., STRENK L.M., MUNOZ P., GRONLUND-JACOB J., DEMARCO J.K., *Age-related changes in human ciliary muscle and lens: a magnetic resonance imaging study*, Investigative Ophthalmology and Visual Science, 1999, 40(6), 1162–1169.
- [17] SVETLOVA O.V., KOSHITZ I.N., *Modern biomechanical ideas about the Helmholtz theory of accommodation*, [in:] E.N. Iomdina and I.N. Koshitz (editors), *Transactions: Ocular Biomechanics*, 156–173, Moskow Helmholtz Research Institute for Eye Diseases, April 2001.
- [18] Van ALPHEN G.W.H.M., GRAEBEL W.P., *Elasticity of tissues involved in accommodation*, Vision Research, 1991, 31(7/8), 1417–1438.
- [19] Von HELMHOLTZ H., *Physiological optics*, Vol. 1, New York, Dover, 1962, pp. 142–172. English translation by J.P.C. Southall for the Optical Society of America (1924) from the 3rd German edition of *Handbuch der Physiologischen Optik*, Hamburg, Voss, 1909.